

Suppression of thermal conduction in non-cooling flow clusters

Biman B. Nath

Raman Research Institute, Bangalore 560080, India
(*biman@rri.res.in*)

7 February 2020

ABSTRACT

Recent X-ray observations have revealed a universal temperature profile of the intracluster gas of non-cooling flow clusters which is flat for $r \leq 0.2r_{180}$. Numerical simulations, however, obtain a steeper temperature profile in the inner region. We study the effect of thermal conduction on the intracluster gas in non-cooling flow clusters in light of these observations, using the steep temperature profiles obtained by authors of numerical simulations. We find that given 10^{10} yr for the intracluster gas to evolve, thermal conduction should be suppressed from the classical value by a factor $\sim 10^{-3}$ in order to explain the observations.

Key words: Cosmology: Theory—Galaxies: Intergalactic Medium—Galaxies : clusters : general—X-rays: Galaxies: Clusters

1 INTRODUCTION

The role of thermal conduction in the intracluster medium has long remained uncertain. For clusters of galaxies which show signs of cooling flow, it has been invoked in the past (Bertschinger & Meiksin 1986; David, Hughes & Tucker 1992) to allow multiphase cooling flows to exist, although the degree of conduction was assumed to be suppressed below the classical value (Binney & Cowie 1981), possibly as a result of tangled magnetic fields (e.g. Fabian 1994). In view of the recent observations of cooling flows, several authors have revived the idea of thermal conduction, albeit with a suppression factor of only a few (Narayan & Medvedev 2001; Voigt et al. 2002).

Concurrently, there have been two important developments in regard to the temperature profile of non-cooling flow clusters. On one hand, observations with *BeppoSAX* have revealed a universal temperature profile, normalised by the emission weighted temperature of the whole cluster, which shows flattening within $r \leq 0.2r_{180}$ (Molendi & de Grandi 2001). On the other hand, numerical simulations obtain a universal temperature profile that is somewhat steeper in this inner region (Loken et al. 2002). One obvious physical mechanism that can flatten the temperature profile and that has not been included in the simulation is thermal conduction (Suginohara & Ostriker 1998; Molendi & de Grandi 2002; Loken et al. 2002).

Recently Loeb (2002) have argued on the basis of comparison of conduction timescale with the age of clusters that thermal conduction should be suppressed at least by a factor ~ 0.15 in order not to allow drastic cooling of the gas in the

cluster cores (of non-cooling flow clusters). Ettori & Fabian (2000) argued that the observed temperature jumps in the cluster A2142 require the thermal conduction across cold fronts should be suppressed by a factor larger than ~ 100 . Vikhlinin et al. (2001) also argued in favour of a suppression factor of ~ 100 . Even in the bulk of the gas, Markevitch et al. (2002) pointed out that a suppression factor larger than ~ 10 is needed to explain the existence of small scale inhomogeneities in the temperature profile of some clusters.

The physical mechanism for and the degree of suppression are still unclear though. The proposed mechanisms include tangled magnetic field (Tribble 1989), plasma instabilities (Pistinner, Levinson & Eichler 1996, and references therein). In the case of suppression by fluctuations in the magnetic field, Chandran & Cowley (1998) found a suppression factor of order 10^{-2} – 10^{-3} . Pistinner, Levinson & Eichler (1996) also advocated an inhibition factor of order $\sim 10^{-3}$ as a result of electromagnetic instabilities. Recently Narayan & Medvedev (2001) extended the analysis of Chandran & Cowley (1998) adding more wavevectors to the fluctuation spectrum of magnetic fields and found a suppression factor of order ~ 5 .

In this paper, we calculate the time evolution of the temperature profile of the intracluster gas in non-cooling flow clusters in the presence of thermal conduction, with various degrees of suppression, assuming quasi-hydrostatic equilibrium, and constrain the suppression factor by comparing the resulting temperature profile with the *BeppoSAX* data.

We first discuss the temperature and density profiles of the intracluster medium and the role of thermal conduction

in §2. We then compare the conduction timescale with the age of clusters in §3. We present the main result of our work in §4. Throughout the paper, we use the Λ CDM cosmological model, with $\Omega_m = 0.3$, $\Omega_\Lambda = 0.7$ and $h = 0.65$.

2 HEAT CONDUCTION AND THE INTRACLUSTER GAS

Heat is conducted along the gradient of the electron temperature in a plasma. Thermal conduction is termed unsaturated if the mean free path of electrons is smaller than the scale length of the temperature gradient. It is said to ‘saturate’ otherwise. In the case of unsaturated thermal conduction, the heat flux is given by,

$$\mathbf{Q} = -\kappa \nabla T_e, \quad (1)$$

where the thermal conductivity of a hydrogen plasma is given by (Spitzer 1962),

$$\kappa_{sp} = 1.8 \times 10^{-5} T_e^{5/2} (\ln \Lambda)_e^{-1} \text{erg s}^{-1} \text{cm}^{-1} \text{K}^{-1}, \quad (2)$$

where the Coulomb logarithm is (Sarazin 1986) (with n_e as the electron density),

$$(\ln \Lambda)_e = 37.8 + \ln \left[\left(\frac{T}{10^8 \text{K}} \right) \left(\frac{n_e}{10^{-3} \text{cm}^{-3}} \right)^{-1/2} \right]. \quad (3)$$

In the case of intracluster gas, we will find that the scale length of the temperature gradient for the relevant temperature profile is larger than the mean free path of electrons ($\sim 23 \text{kpc} (T/10^8 \text{K})^2 (n_e/10^{-3} \text{cm}^{-3})^{-1}$ (Sarazin 1986)) in general. This means that the above mentioned expression for unsaturated heat flux is relevant here. In fact, with the suppression of thermal conduction, as is discussed below, the mean free path is smaller than the above value, bolstering the case for unsaturated heating due to thermal conduction.

Thermal conduction will tend to transport heat from the hotter (usually the inner) regions of the intracluster gas to the colder (usually outer) parts. If the speed of the ensuing gas flow is assumed to be slow, or, equivalently, if the gas density profile is assumed to be in an approximate stationary state, then one can write,

$$\frac{3}{2} \frac{\rho_g(r) k_B}{\mu m_p} \frac{\partial T(r, t)}{\partial t} = -\nabla \cdot \mathbf{Q} = \nabla \cdot (\kappa \nabla T(r, t)), \quad (4)$$

where $\rho_g(r)$, k_B , μ , m_p are the gas density, Boltzmann constant, mean molecular weight and the proton mass respectively.

2.1 Temperature profile

Recently, Molendi & de Grandi (2002) have used the observations of ten non-cooling flow clusters with *BeppoSAX* to derive a universal temperature profile of the intracluster gas. They have normalised the profiles by the emission weighted temperature of the cluster, and plotted the profiles as a function of r/r_{180} , where r_{180} is the radius where the mean overdensity of the cluster is 180 times that of the ambient density. The profiles are characterised by an isothermal core that extends to $r \sim 0.2r_{180}$, beyond which the temperature declines in the outer region.

Molendi & de Grandi (2002) have compared their observed temperature profile with those predicted by several

numerical simulations. Most of the predicted profiles are flatter than the observed profile in the outer region (Evrard et al. 1996; Eke et al. 1998; Bialek et al. 2001). The high resolution simulation by Frenk et al. (1999) did predict a temperature profile that matches well the observed profile in the outer regions. Recently, Loken et al. (2002) have performed a numerical simulation with the highest resolution to date, and determined a universal temperature profile that matches the observed profile of Molendi & de Grandi (2002) very well in the outer region ($r > 0.2r_{180}$). They found a fit to their universal profile that is given by (with $\langle T \rangle$ as the emission weighted temperature), which we use as the initial temperature profile,

$$T_i(r) = \frac{1.33 \langle T_i \rangle}{(1 + \frac{1.5r}{r_{vir}})^{1.6}}. \quad (5)$$

2.2 Gas and dark matter density profile

We assume the gas to be in a quasi-hydrostatic equilibrium state as the temperature profile of the gas evolves. The initial density profile was calculated using the background dark matter density profile of Navarro, Frenk & White (1996) assuming hydrostatic equilibrium. The dark matter density profile is then given by,

$$\rho_{dm}(r) = \rho_s \frac{1}{(r/r_s)(1 + r/r_s)^2}, \quad (6)$$

where ρ_s is a normalizing density parameter. The characteristic radius r_s is related to the virial radius r_{vir} by the ‘concentration parameter’ (c), as

$$c \equiv \frac{r_{vir}}{r_s}. \quad (7)$$

The total mass of the cluster is assumed to be the mass inside its virial radius. The virial radius is calculated in the spherical collapse model to be,

$$r_{vir} = \left[\frac{M_{vir}}{(4\pi/3) \Delta_c(z) \rho_c(z)} \right]^{1/3}, \quad (8)$$

where $\Delta_c(z)$ is the spherical overdensity of the virialized halo within r_{vir} at z in the units of the critical density of the universe $\rho_c(z)$. For our adopted cosmological model $\Omega_m = 0.3$ and $\Omega_\Lambda = 0.7$, the value of $\Delta_c(z)$ is 100 (Komatsu & Seljak 2002). The total dark matter mass within a radius r is

$$M(\leq r) = 4\pi \rho_s r_s^3 m(r/r_s), \quad (9)$$

where, $m(x) = \ln(1+x) - \frac{x}{1+x}$.

We first determine the initial gas density profile corresponding to the initial temperature profile as discussed above, assuming hydrostatic equilibrium,

$$\frac{d}{dr} \left(\frac{\rho_i(r) k_B T_i(r)}{\mu m_p} \right) = -\rho_i(r) \frac{GM(< r)}{r^2}, \quad (10)$$

where ρ_i is the initial gas mass density and $M(< r)$ is the total mass within a radius r as given by equation (9). We normalize the gas density by requiring the total gas mass (within r_{vir}) to be a fraction $f_g = \Omega_b/\Omega_m = 0.15$ of the total mass of the cluster, where we have used $\Omega_b = 0.02h^{-2}$ as constrained by primordial nucleosynthesis (Burles & Tytler 1998).

3 COMPARISON OF TIME SCALES

One can define a conduction time scale for a spherically symmetric cluster as (Sarazin 1986; Sugimotohara & Ostriker 1998; Loeb 2002),

$$t_{cond} = \frac{3}{2} \frac{n_e k_B T}{|\nabla \cdot (\kappa \nabla T)|} = \frac{3}{2} \frac{n_e k_B T}{|\frac{1}{r^2} \frac{d}{dr} (r^2 \kappa \frac{dT}{dr})|}. \quad (11)$$

This can be compared with the age of the cluster, which we assume to be 10^{10} yr (as in, e.g., Loeb 2002). Here the conduction coefficient κ is supposed to be a fraction η of its classical value κ_{sp} (equation(2)). In Figure 1 we show (by solid lines) this time scale for the case of $\eta = 0.1$ for clusters of masses 5×10^{14} , 10^{15} , $2 \times 10^{15} M_\odot$, as a function of r/r_{vir} , and where the dotted line denotes the age of the clusters. We have used the initial temperature and density profiles as discussed in the preceding section. The discontinuity in the solid lines occur as a result of the modulus in the previous equation. It is seen from the comparison of time scales with 10^{10} yr that for $\eta = 0.1$, thermal conduction plays an important role in determining the temperature profile for $r/r_{vir} \leq 0.1$ – 0.2 for the above range of cluster masses. It could be argued that for the cluster temperature profiles to flatten below $r/r_{vir} \leq 0.2$ in $\sim 10^{10}$ yr, the suppression factor for thermal conduction should be ≤ 0.1 .

Loeb (2002) argued on the basis of a similar comparison—constraining $t_{cond}/10^{10} \text{ yr} \leq 0.3$ at r_{180} —that $\eta \leq 0.15(T/10 \text{ keV})^{-3/2}$ in order for the cluster cores not to have cooled substantially over the last Hubble time. We note here that the emission weighted temperature of clusters is related to the total mass as $M \propto T^{3/2}$ (Evrard et al. 1996), so that the limit on η scales as M^{-1} .

Although the comparison of timescales is a good indicator, a much better limit on the suppression factor is expected from the calculation of the time evolution the temperature profile as a result of thermal conduction. For example, from Figure 1 it is seen that for $\eta = 0.1$, say for a cluster with mass $5 \times 10^{14} M_\odot$, $t_{cond} = 10^{10}$ yr at $r/r_{vir} \sim 0.1$. This only means that the temperature would drop at least by a factor $(1 - e^{-1})$ at that radius. This would, however, mean that the temperature profile would be flat within a radius not simply equal to $r/r_{vir} \sim 0.1$ but considerably larger than this. In other words, in reality the suppression factor could be much smaller than that obtained by a simple comparison of time scales.

4 EVOLUTION OF TEMPERATURE PROFILE

We next determine the evolution of the temperature profile using equation (4) with varying degrees of suppression of the value of κ . For numerical integration of the equation with Crank-Nicholson method, it is helpful to change the variable from T to $T^{7/2}$ because $\kappa \propto T^{5/2}$ (equation(2)). The most natural boundary condition is to keep the temperature at r_{vir} a constant, where the effect of thermal conduction would be minimum. We have therefore integrated equation(4), with the boundary condition that the temperature at r_{vir} is a constant.

To facilitate comparison with the *BeppoSAX* temperature profile, which is normalised by the emission weighted temperature, we have calculated the emission weighted temperature for the time-evolved profiles, within r_{2500} as,

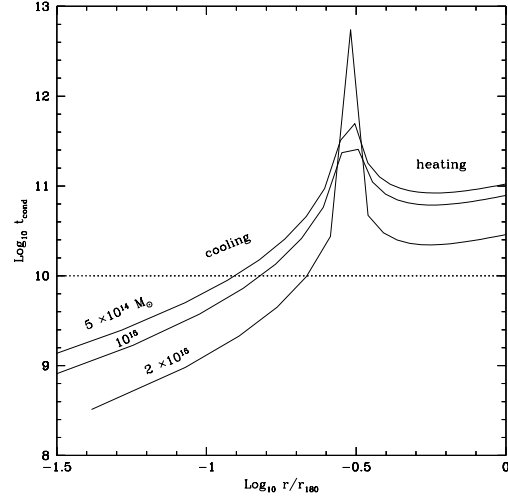


Figure 1. Conduction time scale is compared to the age of the cluster of 10^{10} yr, for three clusters of masses 5×10^{14} , 10^{15} , $2 \times 10^{15} M_\odot$ for a suppression factor of $\eta = 0.1$. The regions of heating and cooling of the gas are marked. The dotted line indicates the timescale of 10^{10} yr that relates to the cluster age.

$$\langle T \rangle = \frac{\int_0^{r_{2500}} 4\pi r^2 n(r)^2 \epsilon_{0.5-10} T(r) dr}{\int_0^{r_{2500}} 4\pi r^2 n(r)^2 \epsilon_{0.5-10} dr}, \quad (12)$$

where n represents gas particle density and $\epsilon_{0.5-10}$ denotes the emissivity for a metallicity of $Z/Z_\odot = 0.3$ relevant for the 0.5–10 keV band, which we calculated using the Raymond-Smith code. We note that the initial profile of Loken et al. (2002), the emission weighted temperature was calculated within a radius of $1 h^{-1}$ Mpc. For this profile, we have adopted the empirical scaling relation of mass and emission weighted temperature of Finoguenov et al. (2001).

We plot in Figure 2 the results of numerically integrating equation (4) beginning with the initial temperature profile of Loken et al. (2002) and the corresponding density profile, computed on the basis of hydrostatic equilibrium. The left panels show the temperature profile at the end of 10^{10} yr for $\eta = 10^{-1}$, 10^{-2} , 10^{-3} (dotted lines) and the right panels show the same for temperature normalized by the corresponding emission weighted temperature. We plot the profiles for $M = 2 \times 10^{15}$ and $5 \times 10^{14} M_\odot$. The mass range is chosen to probe clusters with $\langle T \rangle$ in the range of ~ 4 – 10 keV.

The figures show that given an age of clusters of order $\sim 10^{10}$ yr, a suppression factor for the thermal conduction that is $\eta \gg 10^{-3}$ produces temperature profiles that are flat for a large fraction of the inner region and that are inconsistent with *BeppoSAX* observations. The discrepancies for a given suppression factor become larger for larger clusters, as expected since thermal conduction depends on $T^{5/2}$. It is, however, seen that a value of $\eta \sim 10^{-3}$ results in a temperature profile that is consistent with the *BeppoSAX* data, almost independent of the cluster mass.

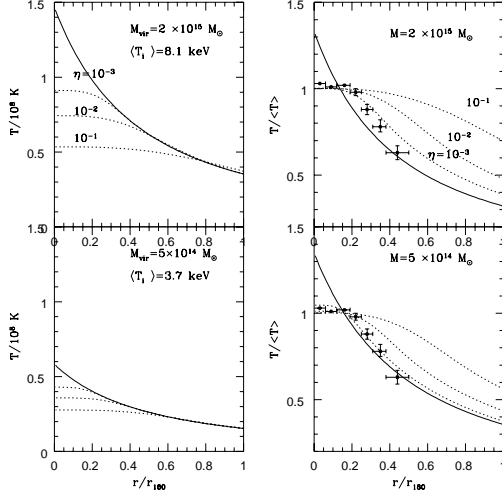


Figure 2. Evolution of the temperature profile is shown for different suppression factors of thermal conduction $\eta = 10^{-1}, 10^{-2}, 10^{-3}$ (dotted lines), beginning with the initial profile shown by the solid line, given 10^{10} yr of evolution, for $M = 2 \times 10^{15} M_{\odot}$ (upper panels) and $M = 5 \times 10^{14} M_{\odot}$ (lower panels). The left panels plot temperature against r/r_{180} and the right panels plot the temperature normalized by the corresponding emission weighted temperature.

5 DISCUSSION

5.1 Luminosity evolution

We can also attempt to constrain the suppression factor from the fact that a substantial evolution in the temperature profile of a cluster over cosmological time scale would also change its X-ray luminosity by a large amount in that time scale. Recent observations, however, find that the X-ray luminosity of clusters scale as $L_x \propto (1+z)^{1.5}$ which is expected from clusters collapsing at various cosmological epochs (see, e.g., Arnaud et al. (2002)). As $L_x \propto \rho^2 R^3 T^{1/2}$, then with $T \propto (\rho R^3)/R$ and $\rho \propto (1+z)^3$, one finds a scaling of L_x at a given temperature with redshift as $(1+z)^{1.5}$. Vikhlinin et al. (2002) found with *CHANDRA* that for a sample of 22 clusters with $z > 0.4$, the X-ray luminosity for a fixed temperature scaled approximately as $(1+z)^{1.5 \pm 0.3}$. If thermal conduction changed the temperature substantially then these observations could be at variance with these simple cosmological scalings.

For the purpose of illustrating the point, consider a cluster of a given mass collapsing at $z = 0.5$, with an initial profile similar to the one we considered in the previous section (and a corresponding density profile from the consideration of hydrostatic equilibrium, taking into account the changes in the dark matter potential and in the fraction Ω_b/Ω_m , appropriate for a collapse redshift of $z = 0.5$). If we now let this cluster passively evolve with thermal conduction at work, then we could track its evolution in the $L_x - T$ space. Vikhlinin et al. (2002) have shown that the data correlate well if the emission weighted temperature is plotted against $L_x \times (1+z)^{1.5}$ (their Figure 2b). In Figure 3, we have plotted the evolutionary track of two representative clusters (of masses 10^{15} and $2 \times 10^{15} M_{\odot}$) from $z = 0.5$ to $z = 0.0$, for the same parameters. We have calculated L_x within a radius

of 2 Mpc and the emission weighted temperature within a shell of 0.5–1 Mpc, as Vikhlinin et al. (2002) have done. We also show the data points from Vikhlinin et al. (2002) as well as their best fit by the dotted line.

The exact calibration of L_x and emission weighted temperature is not important here, as the initial temperature (density) profile has been chosen for the purpose of illustration, not taking into account how the ‘universal’ temperature profile could evolve in redshift. The important points to note in this figure are the extent and direction of the evolutionary tracks. The tracks show how thermal evolution could introduce scatter in this plot. As Voit (2000) has argued the difference between the collapse redshift of a cluster and the redshift at which it is observed can introduce scatter in the plots relating the X-ray parameters.

A small value of thermal conduction coefficient would only move it along the $L_x(1+z)^{1.5}$ axis, mainly because of the redshift factor. Although thermal conduction only conducts heat from the inner to the outer part of the cluster, and on average the gas temperature does not change, but since X-ray emission depends on the density, temperatures determined from X-ray emission would be lowered by thermal conduction. A large value of the coefficient would result in a track in which both L_x and temperature are changed with time. The data at present still have a large scatter and it is not possible to constrain the value of thermal conduction from this, but it might be possible to do so in the near future, if the uncertainties in the temperature measurements decrease the errorbars in the T direction.

Similar evolutionary tracks could also be used for other X-ray parameters, e.g., in the $M - T$ space. The scatter in the data for total mass and the emission weighted temperature, especially for high redshift clusters, such as in Schindler (1999), however is too large to allow any useful constraint on thermal conduction. As Loeb (2002) has pointed out a substantial evolution in the temperature profile would also introduce a large scatter in the measurements of cluster abundance. While these constraints would become better with more data in the future, we have obtained a much stronger limit from the measurement of the temperature profile as described in the previous section.

5.2 Limitations

Finally, we wish to reiterate the basic assumptions made in our calculations to remind ourselves of the limitations of the results. The gas was assumed to be in an approximate steady state condition. We have also done our calculations relaxing this assumption somewhat, by requiring the gas density profile to be in hydrostatic equilibrium at every time step. This did not alter the results much, and we believe that our results should be robust in this regard, as long as there is no large scale gas flow. It should also be pointed out that we have assumed a single value of the suppression factor for the whole of the intracluster gas, independent of density or temperature.

We assumed the intracluster gas to evolve passively in time, without any cooling and heating sources acting in it. It is possible that heating sources, such as active galactic nuclei (Böhringer et al. 2002), which could be more prevalent in the inner region, could compensate the cooling due to thermal conduction in this region to some extent. When radiative

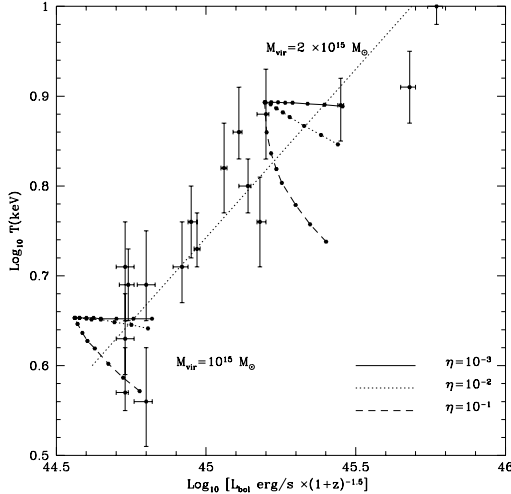


Figure 3. Evolution of a cluster collapsing at $z = 0.5$ in the space of $L_x \times (1+z)^{-1.5}$ and emission weighted temperature is shown for two clusters with $M = 10^{15}$ and $2 \times 10^{15} M_\odot$. Solid, dotted and dashed lines show the evolution for $\eta = 10^{-3}, 10^{-2}, 10^{-1}$. Filled circles along the tracks indicate the luminosity and temperature at $z = 0.5, 0.45, 0.4, 0.35, 0.2, 0.1, 0.0$; the point of convergence of tracks refers to $z = 0.5$. Data points and the dotted line is from Vikhlinin et al. (2002).

cooling is dominant in the central region, as in cooling flow clusters, the direction of heating due to thermal conduction may reverse from being outward to inward. The central region would then heat instead of getting cooled as discussed earlier in the paper. As a matter of fact, it has been speculated that radiative cooling may change the structure of the magnetic field and decrease the suppression of thermal conduction in the central region (Soker & Sarazin 1990). It is also possible that both AGN heating and radiative cooling are important in cooling flow clusters; Ruszkowski & Begelman (2002) found that heating due to thermal conduction suppressed only to the extent of $\eta \sim 0.1$, combined with AGN heating, may explain the recent observations of cooling flow clusters.

We have also implicitly assumed the suppression factor to be homogenous throughout the intracluster gas, which may not always be valid, especially when cooling is important (see above). Fabian, Voigt and Morris (2002) have discussed the possibility that conduction is stronger in the central region than in the outer radii owing to the change in the structure of magnetic fields brought about by cooling in the centre.

6 SUMMARY

We have determined the time evolution of the temperature profile as a result of thermal conduction in the limit that the density profile is in steady state, beginning with temperature profiles obtained from numerical simulations (with thermal conduction). We have constrained the suppression factor for the thermal conduction to be of order $\leq 10^{-3}$ by comparing the final temperature profile (after 10^{10} yr) with the observed profiles. We have also calculated the corresponding evolution of the X-ray luminosity of clusters at

a given temperature, but found the observed data too scattered to allow any useful constraint on thermal conduction.

Acknowledgement It is a pleasure to thank Dipankar Bhattacharya, David Eichler and Abraham Loeb for stimulating discussions and comments on the manuscript. The comments of the anonymous referee have also improved the paper, and they are acknowledged with thanks.

REFERENCES

- Arnaud, M. & Evrard, A. 1999, MNRAS, 305, 631
- Arnaud, M., Aghanim, N. & Neumann, D. M. 2002, A&A, 389, 1
- Bertschinger, E. & Meiksin, A. 1986, ApJ, 306, 1
- Bialek, J. J., Evrard, E. E., & Mohr, J. J. 2001, ApJ, 555, 597
- Binney, J., & Cowie, L. L. 1981, ApJ, 247, 464
- Burles, S. & Tytler, D. 1998, ApJ, 507, 732
- Chandran, B. D. G. & Cowley, S. C. 1998, PRL, 80, 3077
- David, L. P., Hughes, J. P. & Tucker, W. H. 1992, ApJ, 394, 452
- de Grandi, S. & Molendi, S. 2002, ApJ, 567, 163
- Eke, V. R., Navarro, J. F., & Frenk, C. S. 1998, ApJ, 503, 569
- Ettori, S. & Fabian, A. 2000, MNRAS, 317, L57
- Evrard, A., Metzler, C. A. & Navarro, J. F. 1996, ApJ, 469, 494
- Fabian, A. C. 1994, ARAA, 32, 277
- Fabian, A. C., Voigt, L. M. & Morris, R. G. 2002, MNRAS, 335, L71
- Finoguenov, A., Reiprich, T. H., Böhringer, H. 2001, A&A, 368, 749
- Frenk, C. S., et al. 1999, ApJ, 525, 554
- Komatsu, E. & Seljak, U. 2002, MNRAS, 327, 1353
- Loeb, A. 2002, NewA, 7, 279
- Loken, C., Norman, M. L., Nelson, E., Burns, J., Bryan, G. & Motl, P. 2002, ApJ, in press (astro-ph/0207095)
- Markevitch, M. 1998, ApJ, 504, 27
- Markevitch, M., Vikhlinin A. & Forman, W. R. 2002, in ‘Matter and Energy in Clusters of Galaxies’, ASP Conference Series, Vol. X, Eds. S. Bowyer & C. Y. Hwang (in press) (astro-ph/0208208)
- Narayan, R. & Medvedev, M. V. 2001, ApJ, 562, 129
- Navarro, J. F., Frenk C. S., White S. D. M. 1996, ApJ, 462, 563
- Pistinner, S., Levinson, A. & Eichler, D. 1996, ApJ, 467, 162
- Ruszkowski, M. & Begelman, M. C. 2002, ApJ, 581, 223
- Sarazin, C. L. 1986, X-Ray Emission from Clusters of Galaxies (Cambridge: Cambridge Univ. Press)
- Schindler, S. 1999, A&A, 349, 435
- Soker, N. & Sarazin, C. 1990, ApJ, 348, 73
- Spitzer, L., Jr. 1962, Physics of Fully Ionized Gases (2d ed.; New York: Interscience)
- Suginohara, T. & Ostriker, J. P. 1998, ApJ, 507, 16
- Suto, Y., Sasaki, S. & Makino, N. 1998, ApJ, 509, 544
- Tribble, P. C. 1989, MNRAs, 238, 124
- Vikhlinin, A., Markevich, M., Forman, W. & Jones, C. 2001, ApJ, 555, L87
- Vikhlinin, A., VanSpeybroeck, L., Markevitch, M., Forman, W. R. & Grego, L. 2002, ApJ, 578, L107
- Voigt, L. M., Schmidt, R. W., Fabian, A. C., Allen, S. W., Johnstone, R. M. 2002, MNRAS, 335, L7
- Voit, G. M. 2000, ApJ, 543, 113